The 2019 World Congress on
Advances in Structural Engineering and Mechanics (ASEM19)
Jeju Island, Korea, September 17 - 21, 2019

Compression tests on cold-formed steel built-up box sections

*Krishanu Roy[1)], Hieng Ho Lau [2)], Boshan Chen[3)], Tina Chui Huon Ting [4)] and James B.P. Lim [5)]

[1), 3), 5)] *Department of Civil and Environmental Engineering, The University of Auckland, New Zealand*
[2)]*Faculty of Engineering, Computing & Science, Swinburne University of Technology, Sarawak Campus, Kuching, Sarawak, Malaysia*
[4)] *Faculty of Engineering and Science Curtin University Sarawak, Miri, Sarawak, Malaysia*

[1)] kroy405@aucklanduni.ac.nz

ABSTRACT

Built-up box sections are becoming increasingly popular as column members in cold-formed steel (CFS) structures; uses of such sections include CFS trusses, space frames, and portal frames. In this paper, the built-up box sections are fabricated by two identical lipped channel-sections connected at their flanges with self-drilling screws. This paper presents an experimental investigation on the axial capacity of CFS built-up box sections. Compression tests were conducted for different values of slenderness's covering stocky to slender columns. In total 8 built-up box columns were tested. For comparison, 8 single channel sections were also tested and reported herein. Prior to the compression tests, material properties and initial imperfections were measured for both the single channel and CFS built-up box sections. Load-axial shortening relationship, failure modes, and deformed shapes at failure are discussed for CFS built-up box columns. Test results show that all short columns failed through local buckling. However, for slender columns global buckling was observed. The experimental test results were also compared against the designed strength calculated in accordance with the AISI & AS/NZS. From the comparison, it was found that the AISI & AS/NZS are conservative by around 15-19% on average, while predicting the axial capacity of such CFS built-up slender columns.

1. INTRODUCTION

Structural applications for cold-formed steel (CFS) sections are increasing steadily and the use of CFS built-up box sections is becoming popular. This paper presents the results of 16 new experimental tests; of which 8 tests were conducted on CFS built-up box columns, whereas the remaining 8 tests were conducted on single channel sections. The cross-sectional details of the CFS built-up box section are shown

[1)] PhD Scholar
[2)] Professor
[3)] PhD Scholar
[4)] Lecturer
[5)] Professor

in Figure 1. As can be seen, the built-up box section is formed from two identical lipped channel-sections connected front-to-front by self-drilling screws. In such an arrangement, independent buckling of the individual channel-sections is prevented by the screws. Such CFS built-up box sections are used in CFS construction due to the advantages of high load-carrying capacity, stability, and higher moment of inertia, when compared to the back-to-back built-up CFS channel sections.

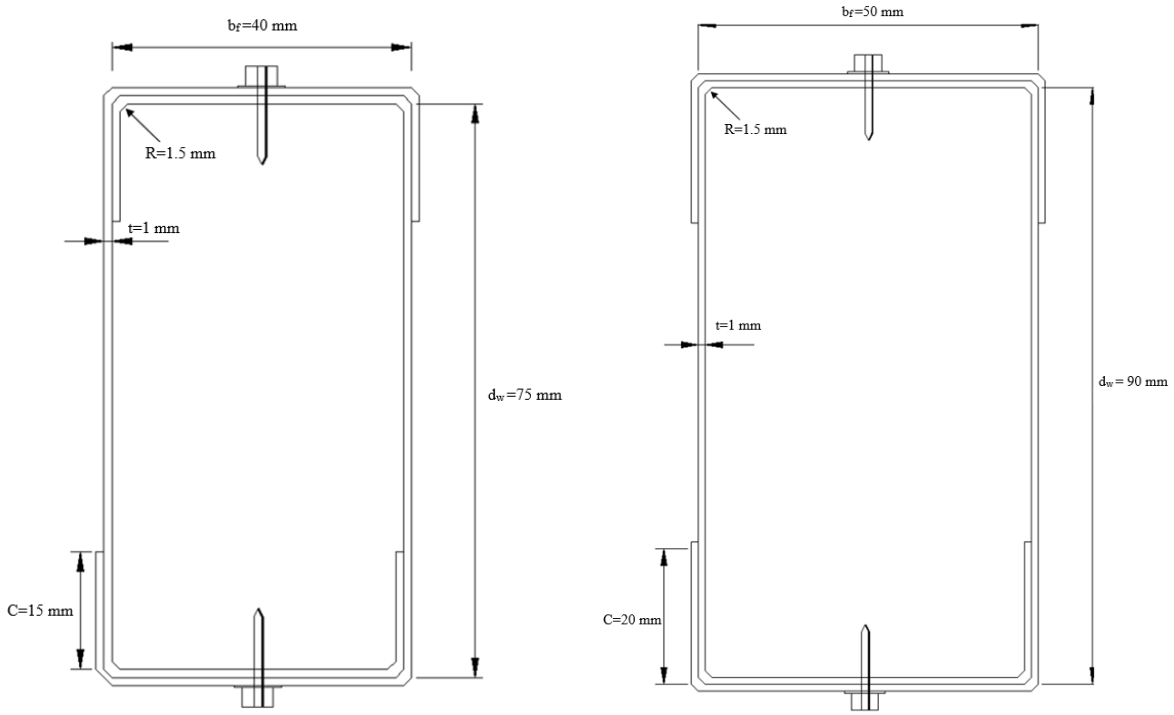

(a) B75 (b) B90

Fig. 1: Nominal cross-sections of CFS built-up box sections considered in this paper

In the literature, no previous work has described any built-up box sections, composed of channels, connected front-to-front through bolts or screws, under axial compression. While Reyes *et al*. (2011) did describe experimental tests on front-to-front channels, these were welded. It was shown that if the seam weld spacing was less than or equal to 600 mm, a modified slenderness ratio could be used instead of the actual slenderness ratio for materials 1.5 mm and 2.0 mm thick. On the other hand, Li *et al.* (2016) conducted experimental and numerical investigations on flexural strength of CFS thin-walled beams with built-up box section which consists of nested C and U sections with the self-drilling screws. For U section beam bending about strong axis, the failure was more “local” than that of C section beams. Craveiro *et al.* (2016) presented an experimental investigation on the fire behaviour of compressed CFS columns with closed built-up cross sections. The investigation by Craveiro *et al.* (2016) suggested that an increase in the non-dimensional axial restraint ratio and column load levels lead to a decrease in critical temperatures.

Some literature is available for research on CFS built-up channels under axial compression, including recent work of the authors (Roy *et al*. 2018a, b, c, d, 2019a,b, c, d). Ting *et al*. (2018) studied the behaviour of CFS built-up channels, connected back-to-back under axial compression (Figure 2 (a)). To extend this work, Roy *et al*. (2018b)

experimentally investigated the axial capacity of CFS built-up channels, connected back-to-back with a gap (Figure 2 (b)). Recently, Roy *et al.* (2018 a) presented a FE investigation on the axial capacity of CFS built-up un-lipped channels screwed back-to-back, concluding that AISI & AS/NZS can be un-conservative for stub columns (Figure 2(c)). Georgieva *et al.* (2012) investigated built-up zed-sections which were connected toe-to-toe (Figure 2(d)). Zhang and Young (2012) studied the compression capacity of built-up channels connected back-to-back with an opening (Figure 2(e)). It should be noted that most of the researchers as discussed above, focussed on the behaviour of back-to-back built-up channels because of the ease in connection between the back-to-back channels.

CFS built-up battened columns were investigated by Dabaon *et al.* (2015), they have concluded that the AISI & AS/NZS and the Eurocodes were un-conservative for columns undergoing local buckling, but the standards predicted the failure load safely for those built-up columns failed by global buckling. Stone and LaBoube (2005) considered stiffened flange and track channels connected back-to-back. Following on from this, Whittle *et al*. (2009) tested the axial capacity of built-up channels which were welded toe-to-toe. Also, Piyawat et al. (2013) investigated welded back-to-back built-up columns under compression. More recently, other researchers have also made some studies on CFS built-up columns: Fratamico *et al.* (2018) and Anbarasu *et al.* (2014) who investigated the axial strength of sheathed and bare built-up CFS columns and CFS built-up web stiffened batten columns, respectively. Recently, Dar *et al.* (2018) investigated the behaviour of laced built-up CFS columns, through experimental and numerical investigations.

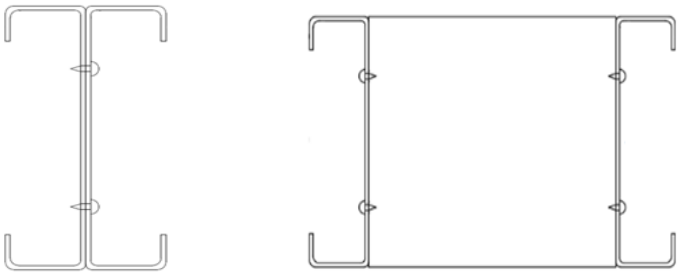

(a) Ting *et al*. (2018) (b) Roy *et al*. (2018b)

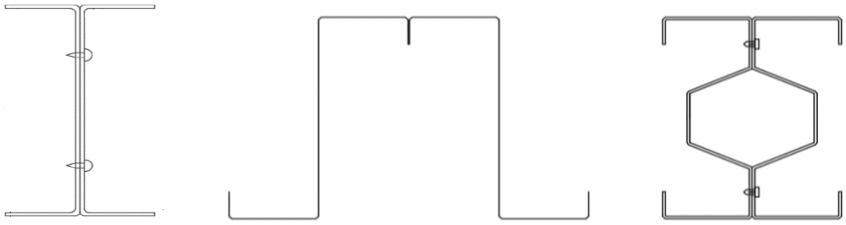

(c) Roy *et al.* (2018 (d) Georgieva *et al.* (2012) (e) Zhang and Young (2012)

Fig. 2: Built-up cold-formed steel columns from literature

Current design guidelines as per the American Iron and Steel Institute AISI and Australia/New Zealand Standard AS/NZS (recommends the use of a modified

slenderness approach to consider the spacing of fasteners while calculating the axial capacity of CFS built-up box sections. It is worth mentioning that the applicability and validity of the modified slenderness method, which has been adopted from the design of hot-rolled steel, has never been demonstrated for CFS built-up box sections.

In total, 16 experimental tests were conducted and reported; 8 of which were for single channel sections (C75) and the remaining 8 tests were for built-up box sections (B75). The nominal cross-sectional geometry of the CFS built-up box columns investigated in this paper is shown in Figure 1. Two different lengths were considered for experimental tests. The material properties and initial imperfections were measured for all test specimens. The effects of slenderness, fastener spacing, load-deflection, load-axial strain behaviour were observed and discussed in detail for different lengths of the columns.This paper has therefore presented an experimental investigation on axial capacity of the CFS built-up box sections.

2. EXPERIMENTAL INVESTIGATION

2.1 Test specimens

Cross-sectional details of the CFS single channel and built-up box sections considered in this paper: C75, and B75, are shown in Figure 1. As can be seen, B75 is the built-up box section from C75 channels. In this study, intermediate fasteners were used to connect the flanges of the front-to-front channels to form the built-up box section. In Figure 3, fastener spacing's for CFS built-up box sections of different lengths are shown. The dimensions of the built-up box sections and single channel sections are summarized in Table 1. The built-up columns were subdivided into two different column heights: short columns of 0.5 m height and slender columns of 1.5 m height. The reason behind choosing such lengths was to capture different buckling failure modes (Local, Distortional and Global buckling) (Ting *et al.* 2018, Roy *et al.* 2018 a, b) of the CFS built-up box sections. Pin-ended boundary conditions were applied for all single channel and built-up columns tested herein. In the test programme, longitudinal screw spacing of 100 mm was considered for all columns.

Table 1 Cross sectional dimensions of the test specimens

(a) C75 (Single lipped channel section)

Specimen	Web d_w (mm)	Flange b_f (mm)	Lip C (mm)	Length L (mm)	Radius R (mm)	Thickness t (mm)
Short						
C75- L500-1	75.0	38.1	14.0	500.2	1.5	1.0
C75- L500-2	76.1	40.0	14.1	501.1	1.5	1.0
C75- L500-3	75.4	39.4	15.2	503.2	1.5	1.0
C75- L500-4	74.8	39.4	15.6	499.7	1.5	1.0
Slender						
C75- L1500-1	76.3	41.2	15.4	1500.1	1.5	1.0
C75- L1500-2	74.7	40.6	14.7	1502.4	1.5	1.0

C75- L1500-3	75.4	39.7	16.1	1498.4	1.5	1.0
C75- L1500-4	74.8	39.2	15.8	1507.2	1.5	1.0

(b) B75 (Built-up box section)

Specimen	Web d_w (mm)	Flange b_f (mm)	Lip C (mm)	Length L (mm)	Radius R (mm)	Thickness t (mm)
Short						
B75- L500-1	76.1	39.8	15.1	500.4	1.5	1.0
B75- L500-2	75.2	38.5	14.2	498.7	1.5	1.0
B75- L500-3	74.7	41.6	14.8	499.6	1.5	1.0
B75- L500-4	77.2	40.2	14.2	502.4	1.5	1.0
Slender						
B75- L1500-1	77.4	41.2	14.4	1500.9	1.5	1.0
B75- L1500-2	76.4	40.6	14.6	1502.6	1.5	1.0
B75- L1500-3	75.4	39.7	15.3	1507.4	1.5	1.0
B75- L1500-4	75.2	38.7	15.1	1511.4	1.5	1.0

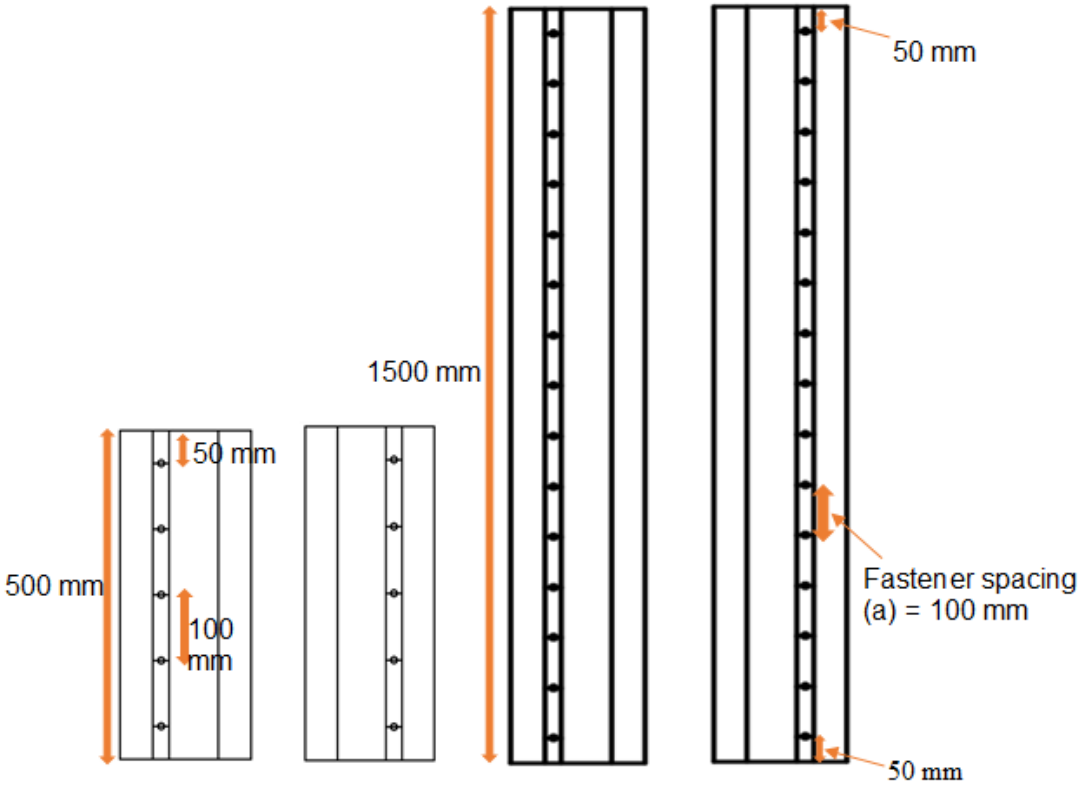

(i) Front facing (ii) Back facing (i) Front facing (ii) Back facing

(a) Short column (b) Slender column

Fig. 3: Fastener spacing– for the built-up box sections used in the experimental tests

2.2 Specimen labelling

Type of the built-up section, nominal specimen length, and test specimen number was coded by the specimen labeling. For example, the label “B75-L1500-1”, as shown in Figure 4, indicates the depth of the channel section is 75 mm. B stands for the built-up box section and L indicates the specimen length as is 1500 mm. At the end of the label, the number 1 is used to express the specimen number as 1. On the other hand, “C75- L1500-1” indicates single channel section with 75 mm web depth, having 1500 mm nominal specimen length and being specimen number 1 (Figure 4(a)). Unlike the specimen labeling used in the experimental program, a different column labeling was used in the parametric study to indicate fastener spacing. As for example, the label “B75-a100-L300-1” indicates the built-up box section with 75 mm web depth, 100 mm fastener spacing having 300 mm nominal specimen length and being specimen number 1.

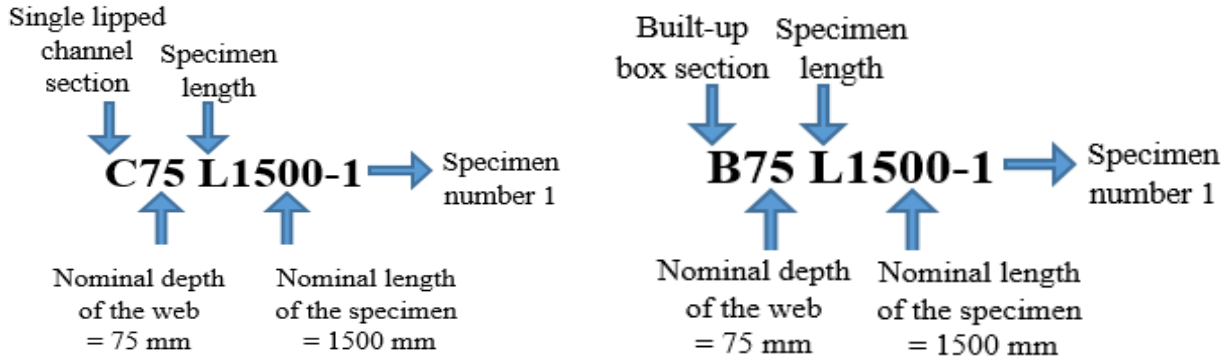

(a) Single lipped channel section (b) Built-up box section

Fig. 4: Specimen labelling

2.3 Tensile coupon tests

In order to determine the material properties of the cold-formed steel, tensile coupons were cut from both the longitudinal and transverse directions. The coupons were laser cut. Five coupons were cut from both longitudinal and transverse directions of the built-up box and single channel sections. All the coupons were then tested according to the British standard BS EN (2001). The width of the coupons was 12.5 mm with a gauge length of 50 mm. A test machine, Instron 4469 which has a capacity of 50 kN, was used to conduct the tensile coupon tests. The load was applied through displacement control. An extensometer was used to record the strain values, which had a gauge length of 50 mm. Average initial and full stress-strain curves of the steel determined from the coupon tests are shown in Figure 5(a) and Figure 5(b), respectively. From the results of tensile coupon tests for longitudinal and transverse coupons, average values of the E and F_y were 207 N/mm^2 and 559 N/mm^2, respectively (Table 2).

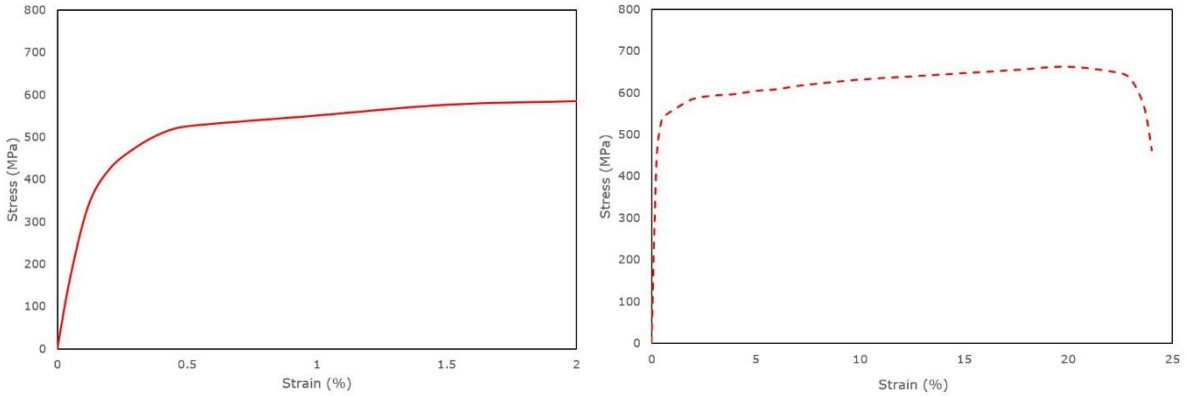

(a) Initial stress–strain curve (b) Full stress–strain curve

Fig. 5: Initial and final stress-strain curves of the CFS used in this research

Table 2 Material properties obtained from tensile coupon tests

Section	Nominal thickness	Base metal thickness	Gauge length	Yield stress	Gauge width	Ultimate stress	Young's modulus
	t	T	L_0	$\sigma_{0.2}$	*b*	σ_u	E
	(mm)	(mm)	(mm)	(MPa)	(mm)	(MPa)	GPa
Longitudinal	1.01	1.0	50	559	12.5	678	207

2.4 Test-rig and testing procedure

All the built-up box sections and single channels were loaded using a Universal Testing Machine (UTM) (Figure 6). The capacity of the UTM was 600 kN. Pin-ended boundary conditions were applied for all single channel and built-up columns tested herein. In order to ensure there was no gap between the two pin-ends and end plates of the specimen, all columns were loaded initially up to 25% of their expected failure load and then released. All columns were loaded under displacement control, with a displacement rate of 0.03 mm/s (Figure 7). Load was applied through the centre of gravity (CG) of the specimens. Four LVDTs were used for all built-up column tests. LVDT positions are shown in Figure 8. One LVDT was used in the longitudinal direction to measure the axial shortening, while all other LVDTs were used in the transverse direction, to measure the lateral displacement of the built-up columns. With each increment of loading, LVDT readings were recorded, until the ultimate failure of single-channel and built-up box sections occurred. A load cell was installed at the top of the base plate, which was used to record the failure load. The axial load and the readings of the transducers were recorded by a data acquisition system at regular intervals during the tests.

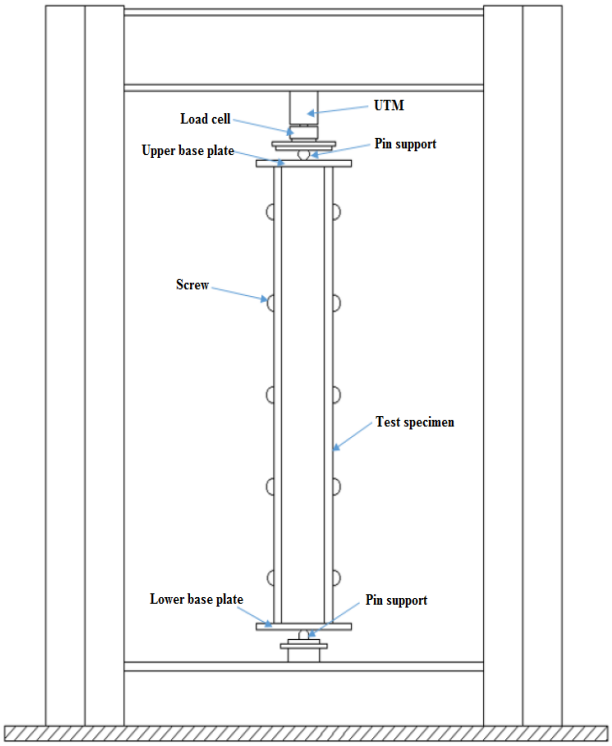

Fig. 6: Drawing of loading test-rig

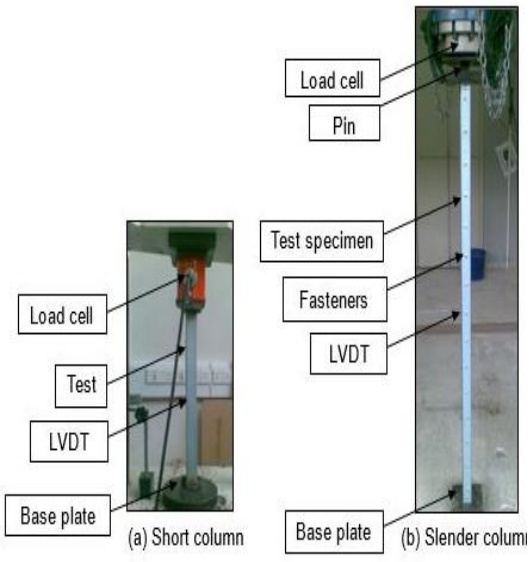

Fig. 7: Test set-up for short and slender columns

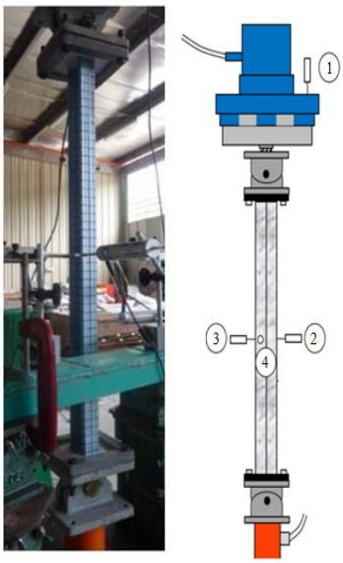

Fig. 8: Position of LVDTs (slender column tests

2.5 Initial imperfections measurement

During construction of CFS structures, geometric imperfections are caused by fabrication and transportation problems. When the CFS built-up columns were transported from the manufacturing site to the testing site, they may have gone through some cross sectional distortions. It is very important to include those geometric imperfections in finite element models to validate the results of experimental tests. An imperfection measurement set-up is shown in Figure 9(a). To measure the initial imperfections of all test specimens, an LVDT, with a precision of 0.001 mm, was used. Initial imperfections were recorded along the centre of the web, flanges, and edges of the lips at every 20 mm along the length of the built-up sections. In Figure 9(b), initial imperfections are plotted against the length of the B75-L500-1. The maximum imperfections of single channels and built-up box sections are shown in Table 3. These values of overall imperfections given in Table 3 were measured in the middle of the flanges, webs and lips of each channel and built-up sections and the average of the maximum values were considered. Although it is expected to have maximum imperfections at the corners and lips for the plain channels and back-to-back built-up channels (Fratamico *et al.* 2018), it was not the case for CFS built-up box sections. The maximum overall imperfections were observed in the middle of the flanges, lips and webs for such CFS built-up box sections. This may be because of the type of box sections (front-to-front connections) and it was observed that the sections buckled in the middle of flange and webs during the transportation of the built-up sections to the testing site. These mean overall imperfections were used in the finite element modeling of a single channel and built-up box sections

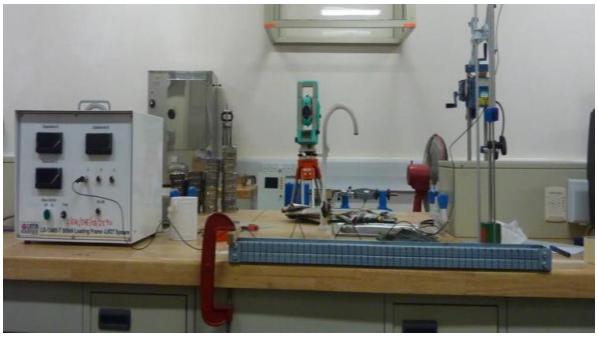

(a) Imperfection measurement setup

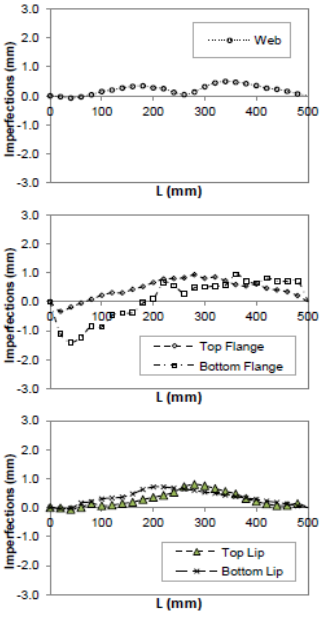

(b) Typical imperfection profile for B75-L500-1

Fig. 9: Details of imperfection measurements from experimental investigation

Table 3 Maximum initial overall imperfections present in single channels and CFS built-up box sections

(a) C75

Specimen	Maximum initial imperfections (mm)
Short	
C75- L500-1	0.36
C75- L500-2	0.58
C75- L500-3	0.45
C75- L500-4	0.47
Slender	
C75- L1500-1	0.66
C75- L1500-2	0.62
C75- L1500-3	0.51
C75- L1500-4	0.59

(b) B75

Specimen	Maximum initial imperfections (mm)
Short	
B75- L500-1	0.16
B75- L500-2	0.18
B75- L500-3	0.15
B75- L500-4	0.17
Slender	
B75- L1500-1	0.23
B75- L1500-2	0.21
B75- L1500-3	0.20
B75- L1500-4	0.18

2.6 Experimental results

Table 4 shows the single channel and built-up column's failure loads determined from the experimental tests (P_{EXP}). As shown in Table 4, significant strength reduction occurred for both single channel and built-up columns for 1500 mm length.

Table 4 Axial capacity of the tested specimens

(a) C75 (Single lipped channel section)

Specimen	Experimental Results	AISI & AS/NZS Design Results	
	P_{EXP} (kN)	P_{AISI} (kN)	P_{AISI}/P_{EXP} -
Short			
C75- L500-1	57.5	53.2	0.93
C75- L500-2	55.5	53.2	0.96
C75- L500-3	54.2	53.2	0.98
C75- L500-4	57.7	53.2	0.92
Mean			0.96
COV			0.03
Slender			
C75- L1500-1	39.0	37.1	0.95
C75- L1500-2	40.5	37.1	0.92
C75- L1500-3	42.0	37.1	0.88
C75- L1500-4	45.5	37.1	0.82
Mean			0.89
COV			0.06

(b) B75 (Built-up box section)

Specimen	Experimental Results	AISI & AS/NZS Design Results	
	P_{EXP} (kN)	P_{AISI} (kN)	P_{AISI}/P_{EXP} -
Short			
B75- L500-1	124.8	115.3	0.92
B75- L500-2	127.5	115.3	0.90
B75- L500-3	130.5	115.3	0.88
B75- L500-4	129.7	115.3	0.89
Mean			0.91
COV			0.02
Slender			
B75- L1500-1	88.4	73.1	0.83
B75- L1500-2	89.7	73.1	0.81
B75- L1500-3	91.4	73.1	0.80
B75- L1500-4	92.7	73.1	0.79
Mean			0.81
COV			0.02

In total, 16 experimental tests were conducted. Of these, 8 tests were conducted on the axial capacity of built-up box sections and the remaining 8 tests were conducted on single channel sections (Table 4). Different buckling modes were observed for 500 mm and 1500 mm length columns. As expected, all built-up short columns failed through local buckling and all slender columns failed by global buckling. However, short columns of single channels failed through either distortional buckling or a combination of local-distortional buckling. Failure modes obtained from the tests are shown in Figures 10(a) and 10(b) for single and built-up box columns, respectively. The Load-displacement curves for short and slender columns are plotted in Figure 11(a) for single channel section columns. Besides, load versus axial shortening behavior of CFS built-up box columns are shown in Figure 11(b). It was noticed that the axial displacement of the built-up box sections increases linearly up to a load of 66.3 kN, which is approximately 75% of the ultimate failure load for B75-L1500-1. After that, nonlinear behavior was noticed until the failure load is reached, which is 88.4 kN. Similar observations were made for other built-up columns (Figure 11(b)). Load-lateral displacements are also plotted for B75-L500-1 and B75-L1500-1 at middle and quarter-length of the built-up column (Figure 12).

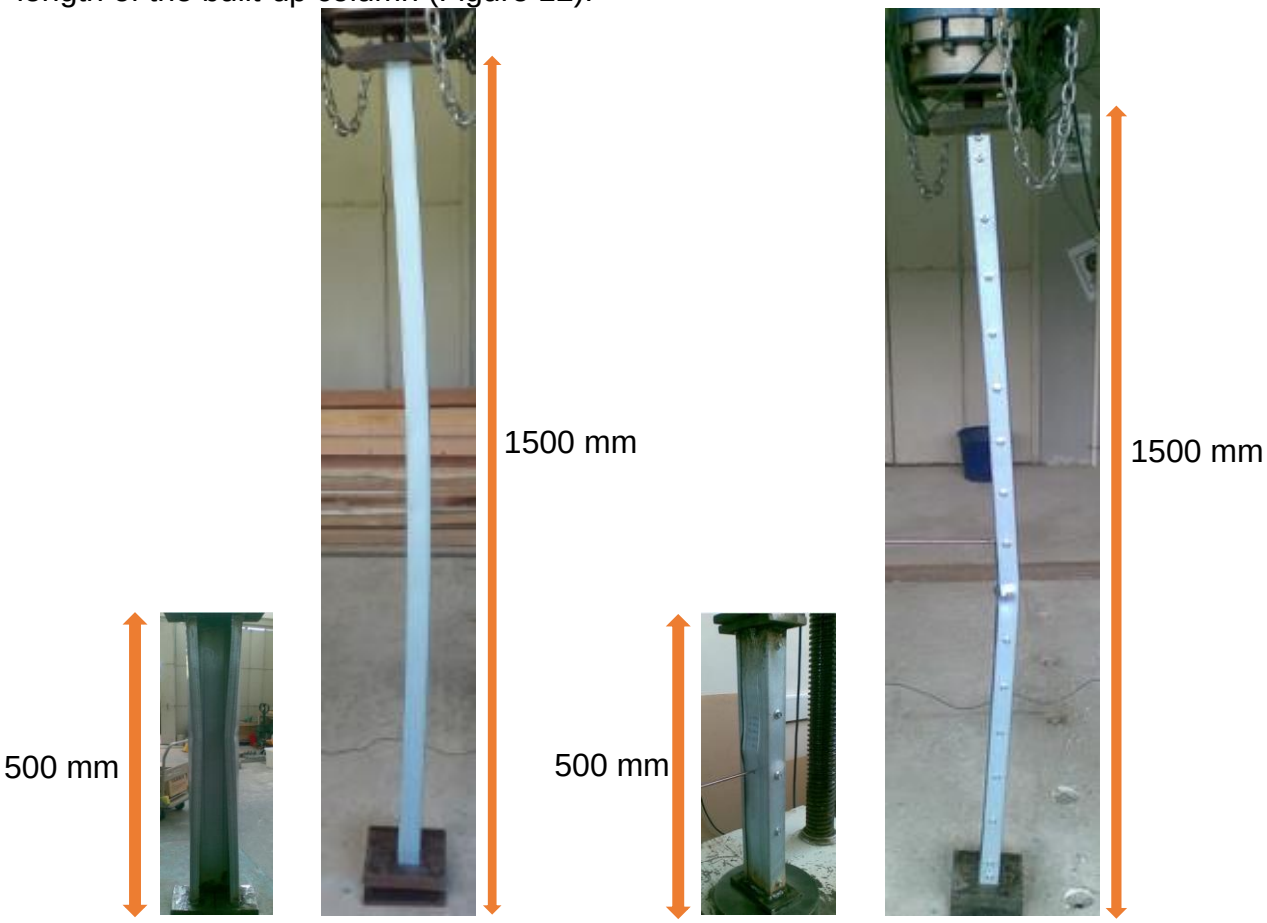

(i) C75-L500-1 (ii) C75-L1500-1 (i) B75-L500-1 (ii) B75-L1500-1

(a) Single channel sections (b) CFS built-up box sections

Fig. 10: CFS single and built-up columns at failure

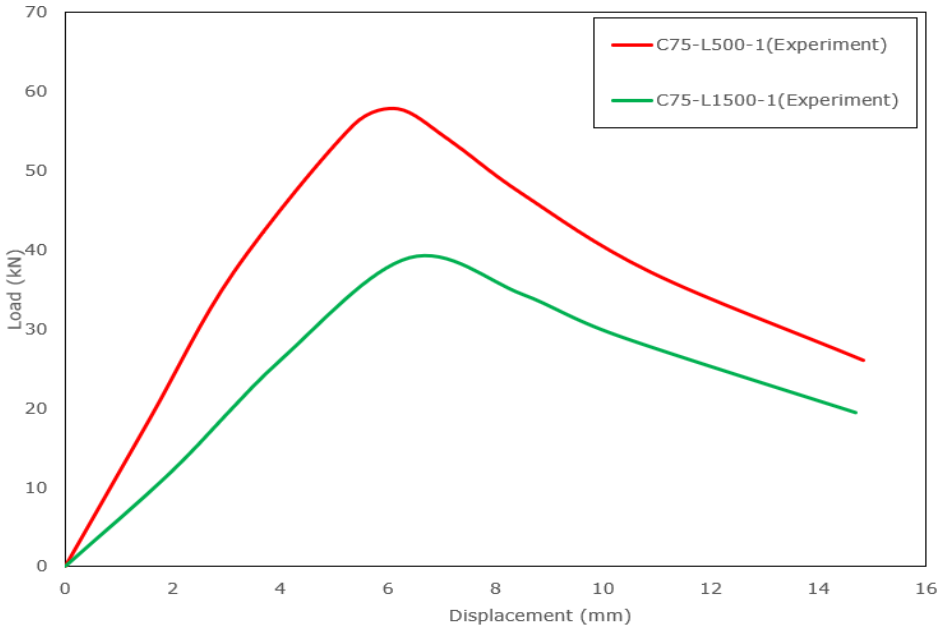

(a) C75

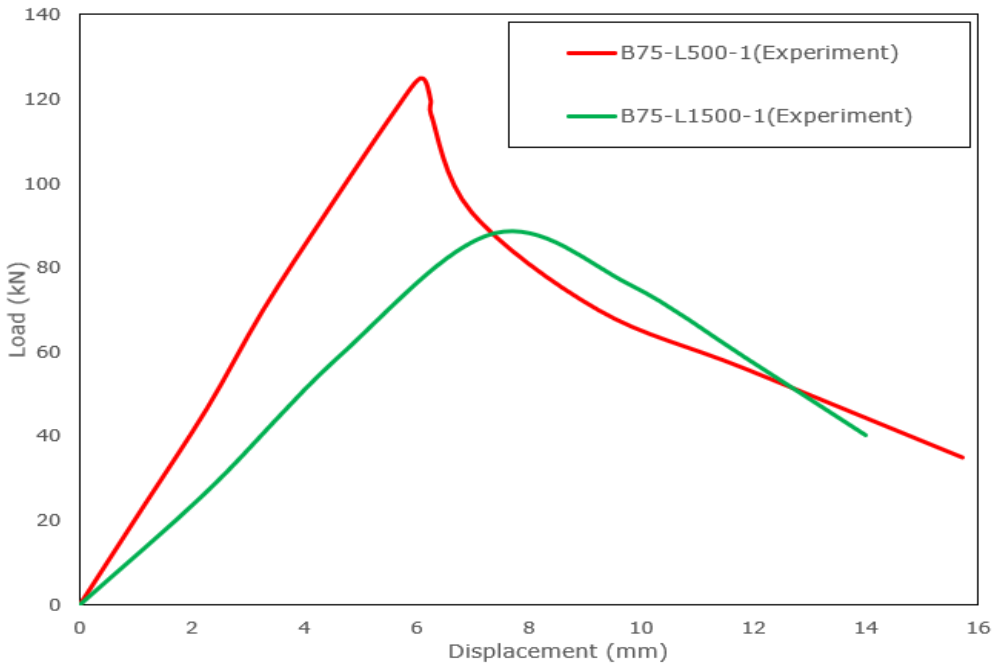

(b) B75

Fig. 11: Load versus axial displacement curves for CFS single channel and built-up box sections

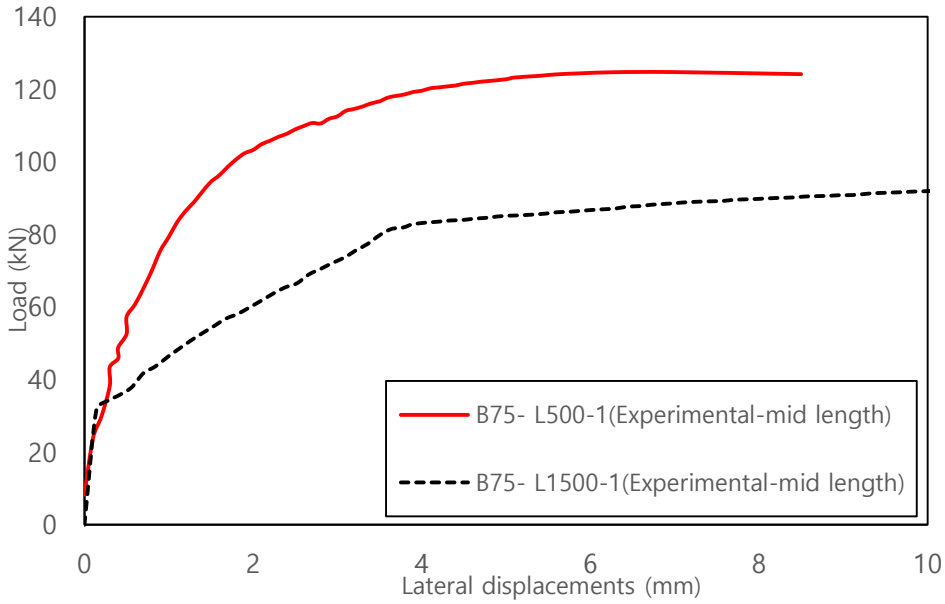

Fig. 12: Load versus lateral displacements relationship for CFS built-up box sections

3. DESIGN STRENGTHS CALCULATED IN FROM THE AISI & AS/NZS

The test strengths were compared against the AISI & AS/NZS design strengths for CFS built-up box sections. The AISI & AS/NZS uses the Effective width method (EWW) while calculating the axial capacity of CFS built-up box columns. According to the AISI (2016) & AS/NZS (2018), for built-up CFS columns, the axial capacity is calculated as follows:

$$P_{AISI\&AS/NZS} = A_e F_n \quad (1)$$

The critical buckling stress (F_n) was determined as below:

For $\lambda_c \leq 1.5$, $F_n = \left(0.658^{\lambda^2 c}\right) F_y$ (2)

For $\lambda_c > 1.5$, $F_n = \left(\frac{0.877}{\lambda^2_c}\right) F_y$ (3)

The non-dimensional slenderness (λ_c) is calculated using Eq. (4):

$$\lambda_c = \sqrt{\frac{F_y}{F_e}} \quad (4)$$

Eq. (1) to Eq. (4) can be found in the AISI (2016) standard in section E2, whereas these equations (Eq. (1) to Eq. (4)) can be found in the AS/NZS (2018) standard in section 3.4.1.

Modified slenderness ratio was used for all calculations as per Eq. (5).

$$\left(\frac{KL}{r}\right)_{ms} = \sqrt{\left(\frac{KL}{r}\right)^2_o + \left(\frac{a}{r_{yc}}\right)^2}\text{; For which } \left(\frac{a}{r_{yc}}\right) \leq 0.5\left(\frac{KL}{r}\right)_o \quad (5)$$

Eq. (5) can be found in the AISI (2016) standard in section I1.2, and in the AS/NZS (2018) standard, this equation (Eq. (5)) can be found in section 4.1.2.

Axial capacities obtained from the AISI & AS/NZS are compared in Table 4 for CFS built-up box columns. The mean values of P_{AISI} / P_{EXP} are 0.91 and 0.81 (Table 4(b)) for the short and slender box columns, respectively. Therefore it can be concluded that the AISI & AS/NZS standards are over-conservative by around 15 to 19%, while predicting the axial capacity of CFS built-up slender columns.

4. CONCLUSIONS

In this paper, an experimental investigation on axial capacity of CFS built-up box sections is presented. For comparison, another 8 single channels were also tested under axial compression. The material properties and initial imperfections were measured for all test specimensFrom the experimental tests, load-axial displacement, load-lateral displacement, load-axial strain relationships and buckling modes at failure are discussed for both the single channel and CFS built-up box sections. The effect of fastener spacing on compression capacity of built-up CFS box sections is also investigated. Test results show that all the built-up short columns failed through local buckling. However, all the slender CFS built-up box columns failed by global buckling. The experimental test results were also compared against the designed strength calculated in accordance with the AISI & AS/NZS. From the comparison, it was found that the AISI & AS/NZS are conservative by around 15-19% on average, while predicting the axial capacity of such CFS built-up slender columns.

REFERENCES

American Iron and Steel Institute (AISI) (2016), “North American Specification for the Design of Cold-formed Steel Structural Members”, AISI S100-16.

Anbarasu, D. M., Kumar, P. B., & Sukumar, D. S. (2014), “Study on the capacity of cold-formes steel built-up battened columns under axial compression”, *Latin American J. Solid. Struct.*, **11**(12), 2271-2283.

Australia/New Zealand Standard (AS/NZS) (2018), “Cold-Formed Steel Structures, AS/NZS **4600:2018**, Standards Australia/ Standards New Zealand.

BS EN (2001), Tensile testing of metallic materials method of test at ambient temperature; British Standards Institution

Craveiro, H. D., Rodrigues, J. P. C., & Laím, L. (2016), “Experimental analysis of built-up closed cold-formed steel columns with restrained thermal elongation under fire conditions”, *Thin-Walled. Struct.*, **107**, 564-579.

Dabaon, M., Ellobody, E., & Ramzy, K. (2015), “Nonlinear behaviour of built-up cold-formed steel section battened columns”, *J. Constr. Steel Res.*, **110**, 16-28.

Dar, M. A., Sahoo, D. R., Pulikkal, S., & Jain, A. K. (2018), “Behaviour of laced built-up cold-formed steel columns: Experimental investigation and numerical validation”, *Thin-Walled. Struct.*, **132**, 398-409.

Fratamico, D. C., Torabian, S., Zhao, X., Rasmussen, K. J., & Schafer, B. W. (2018), “Experimental study on the composite action in sheathed and bare built-up cold-formed steel columns”, *Thin-Walled. Struct.*, **127**, 290-305.

Georgieva, I., Schueremans, L., & Pyl, L. (2012), “Composed columns from cold-formed steel Z-profiles: Experiments and code-based predictions of the overall compression capacity”, *Eng. Struct.*, **37**, 125-134.

Li, Y. L., Li, Y. Q., & Shen, Z. Y. (2016), "Investigation on flexural strength of cold-formed thin-walled steel beams with built-up box section", *Thin-Walled. Struct.*, **107**, 66-79.

Piyawat, K., Ramseyer, C., & Kang, T. H. K. (2013), "Development of an axial load capacity equation for doubly symmetric built-up cold-formed sections", *J. Struct. Eng*., 139(12), 04013008-13.

Reyes, W., & Guzmán, A. (2011), "Evaluation of the slenderness ratio in built-up cold-formed box sections", *J. Constr. Steel Res.*, **67**(6), 929-935.

Roy, K., Ting, T. C. H., Lau, H. H., & Lim, J. B. (2018a), "Effect of thickness on the behaviour of axially loaded back-to-back cold-formed steel built-up channel sections-Experimental and numerical investigation", *Structures*, **16**, 327-346.

Roy, K., Ting, T. C. H., Lau, H. H., & Lim, J. B. (2018b), "Nonlinear behaviour of back-to-back gapped built-up cold-formed steel channel sections under compression", *J. Constr. Steel Res*, **147**, 257-276.

Roy, K., Ting, T. C. H., Lau, H. H., & Lim, J. B. (2018c), "Effect of thickness on the behaviour of axially loaded back-to-back cold-formed steel built-up channel sections-Experimental and numerical investigation", *Proceedings of the 'Wei-Wen Yu International Specialty Conference on Cold-Formed Steel Structures*, St. Louis, Missouri, USA.

Roy, K., Ting, T. C. H., Lau, H. H., & Lim, J. B. (2018d), "Nonlinear behavior of axially loaded back-to-back built-up cold-formed steel un-lipped channel sections", *Steel Compos. Struct*, 28 (2), 233-250.

Roy, K., Ting, T. C. H., Lau, H. H., & Lim, J. B. (2019a), "Experimental and numerical investigations on the axial capacity of cold-formed steel built-up box sections", *J. Constr. Steel Res*, **160**, 411-427.

Roy, K., Mohammadjani, C., & Lim, J. B. (2019b), "Experimental and numerical investigation into the behaviour of face-to-face built-up cold-formed steel channel sections under compression", *Thin-Walled. Struct.*, **134**, 291-309.

Roy, K., Lau, H. H., & Lim, J. B. (2019c), "Numerical investigations on the axial capacity of back-to-back gapped built-up cold-formed stainless steel channels", Adv. Struct. Eng, 22, 2289-2310.

Roy, K. & Lim, J. B. (2019d), "Numerical investigation into the buckling behaviour of face-to-face built-up cold-formed stainless steel channel sections under axial compression", *Struct,* **20**, 42-73.

Stone, T. A., & LaBoube, R. A. (2005), "Behavior of cold-formed steel built-up I-sections", *Thin-Walled. Struct.*, **43**(12), 1805-1817.

Ting, T. C. H., Roy, K., Lau, H. H., & Lim, J. B. (2018), "Effect of screw spacing on behavior of axially loaded back-to-back cold-formed steel built-up channel sections", *Adv. Struct. Eng*, **21**(3), 474-487.

Whittle, J., & Ramseyer, C. (2009), "Buckling capacities of axially loaded, cold-formed, built-up C-channels", *Thin-Walled. Struct.*, **47**(2), 190-201.

W. Reyes, A. Guzman (2011), "Evaluation of the slenderness ratio in built-up cold-formed box sections", *J. Constr. Steel Res*. **67** 929–935.

Zhang, J. H., & Young, B. (2012), "Compression tests of cold-formed steel I-shaped open sections with edge and web stiffeners", *Thin-Walled. Struct.*, **52**, 1-11.